10 Spatial mode transmission using low differential mode delay 6-LP fiber using all-fiber photonic lanterns

John van Weerdenburg,[1] Amado Velàzquez-Benitez,[2] Roy van Uden[1], Pierre Sillard,[3] Denis Molin,[3] Adrian Amezcua-Correa[3], Enrique Antonio-Lopez[2], Maxim Kuschnerov,[4] Frans Huijskens,[1] Hugo de Waardt,[1] Ton Koonen[1], Rodrigo Amezcua-Correa,[2] and Chigo Okonkwo[1,*]

[1]COBRA Research Institute, Eindhoven University of Technology, The Netherlands
[2]CREOL, The College of Optics and Photonics, the University of Central Florida, Orlando, Florida 32816, USA
[3]Prysmian Group, Parc de Industries Artois Flandres, 644 boulevard Est, Billy Berclau, 62092, France
[4]Coriant R&D GmbH, St.-Martin-Str. 76, 81541 Munich, Germany
[*]cokonkwo@tue.nl

Abstract: To unlock the cost benefits of space division multiplexing transmission systems, higher spatial multiplicity is required. Here, we investigate a potential route to increasing the number of spatial mode channels within a single core few-mode fiber. Key for longer transmission distances and low computational complexity is the fabrication of fibers with low differential mode group delays. As such in this work, we combine wavelength and mode-division multiplexed transmission over a 4.45 km low-DMGD 6-LP-mode fiber by employing low-loss all-fiber 10-port photonic lanterns to couple light in and out of the fiber. Hence, a minimum DMGD of 0.2 ns (maximum 0.357 ns) is measured after 4.45 km. Instrumental to the multi-mode transmission system is the employed time-domain-SDM receiver, allowing 10 spatial mode channels (over both polarizations) to be captured using only 3 coherent receivers and real-time oscilloscopes in comparison with 10 for conventional methods. The spatial channels were unraveled using 20 × 20 multiple-input multiple-output digital signal processing. By employing a novel round-robin encoding technique, stable performance over a long measurement period demonstrates the feasibility of 10x increase in single-core multi-mode transmission.

OCIS codes: (030.4070) Modes; (060.4080) Modulation; (060.4510) Optical communications; (060.1660) Coherent communications.

References and links

1. Sandvine, "Global Internet Phenomena Report 2H 2013," 2013.
2. A. M. J. Koonen, H. S. Chen, R. G. H. van Uden, and C. M. Okonkwo, "Compact integrated solutions for mode (de-)multiplexing," in *Proceedings of the 2014 OptoElectronics and Communication Conference (OECC) and Australian Conference on Optical Fibre Technology* (IEEE, 2014), pp. 164–166.
3. M. Kushnerov and V. Sleiffer, "Multi-mode SDM systems: upgrade scenario for legacy systems and achievable system cost," in *Proceedings of the European Conference on Optical Communications* (ECOC, 2013), pp. 1-22.
4. J. Sakaguchi, B. J. Puttnam, W. Klaus, Y. Awaji, N. Wada, A. Kanno, T. Kawanishi, K. Imamura, H. Inaba, K. Mukasa, R. Sugizaki, T. Kobayashi, and M. Watanabe, "305 Tb/s Space Division Multiplexed Transmission Using Homogeneous 19-Core Fiber," J. Lightwave Technol. **31**(4), 554–562 (2013).
5. V. A. J. M. Sleiffer, Y. Jung, V. Veljanovski, R. G. H. van Uden, M. Kuschnerov, H. Chen, B. Inan, L. G. Nielsen, Y. Sun, D. J. Richardson, S. U. Alam, F. Poletti, J. K. Sahu, A. Dhar, A. M. J. Koonen, B. Corbett, R. Winfield, A. D. Ellis, and H. de Waardt, "73.7 Tb/s (96 x 3 x 256-Gb/s) mode-division-multiplexed DP-16QAM transmission with inline MM-EDFA," Opt. Express **20**(26), B428–B438 (2012).

#240465 Received 11 May 2015; revised 31 Jul 2015; accepted 3 Aug 2015; published 11 Sep 2015

6. R. G. H. van Uden, R. A. Correa, E. A. Lopez, F. M. Huijskens, C. Xia, G. Li, A. Schülzgen, H. de Waardt, A. M. J. Koonen, and C. M. Okonkwo, "Ultra-high-density spatial division multiplexing with a few-mode multicore fibre," Nat. Photonics **8**(11), 865–870 (2014).
7. R. Ryf, N. K. Fontaine, M. A. Mestre, S. Randel, X. Palou, C. Bolle, A. H. Gnauck, S. Chandrasekhar, X. Liu, B. Guan, R. Essiambre, P. J. Winzer, S. Leon-Saval, J. Bland-Hawthorn, R. Delbue, P. Pupalaikis, A. Sureka, Y. Sun, L. Grüner-Nielsen, R. V. Jensen, and R. Lingle, "12 x 12 MIMO Transmission over 130-km Few-Mode Fiber," in Frontiers in Optics 2012/Laser Science XXVIII, OSA Technical Digest (online) (Optical Society of America, 2012), paper FW6C.4.
8. N. K. Fontaine, R. Ryf, H. Chen, A. V. Benitez, B. Guan, R. Scott, B. Ercan, S. J. B. Yoo, L. E. Grüner-Nielsen, Y. Sun, R. Lingle, E. Antonio-Lopez, and R. Amezcua-Correa, "30×30 MIMO Transmission over 15 Spatial Modes," in Optical Fiber Communication Conference Post Deadline Papers, OSA Technical Digest (online) (Optical Society of America, 2015), paper Th5C.1.
9. P. J. Winzer and G. J. Foschini, "MIMO capacities and outage probabilities in spatially multiplexed optical transport systems," Opt. Express **19**(17), 16680–16696 (2011).
10. K.-P. Ho and J. M. Kahn, "Mode-dependent loss and gain: statistics and effect on mode-division multiplexing," Opt. Express **19**(17), 16612–16635 (2011).
11. P. Sillard, D. Molin, M. Bigot-Astruc, H. Maerten, D. van Ras, and F. Achten, "Low-DMGD 6-LP-Mode Fiber," in Optical Fiber Communication Conference, OSA Technical Digest (online) (Optical Society of America, 2014), paper M3F.2.
12. P. Sillard, D. Molin, M. Bigot-Astruc, K. de Jongh, and F. Achten, "Low-Differential-Mode-Group-Delay 9-LP-Mode Fiber," in *Optical Fiber Communication Conference*, OSA Technical Digest (online) (Optical Society of America, 2015), paper M2C.2.
13. H. Chen, R. van Uden, C. Okonkwo, and T. Koonen, "Compact spatial multiplexers for mode division multiplexing," Opt. Express **22**(26), 31582–31594 (2014).
14. H. Chen, V. A. J. M. Sleiffer, R. G. H. Van Uden, C. M. Okonkwo, M. Kuschnerov, F. M. Huijskens, L. Grüner-Nielsen, Y. Sun, H. De Waardt, and A. M. J. Koonen, "3 MDMx8 WDMx320 Gb/s DP 32QAM transmission over a 120km few-mode fiber span employing 3-spot mode couplers," Proc. 18th OptoeElectronics and Communications Conference (OECC), paper PD3–6-1 (2013).
15. T. A. Birks, I. Gris-Sánchez, S. Yerolatsitis, S. G. Leon-Saval, and R. R. Thomson, "The photonic lantern," Adv. Opt. Photonics **7**(2), 107–167 (2015).
16. S. G. Leon-Saval, T. A. Birks, J. Bland-Hawthorn, and M. Englund, "Multimode fiber devices with single-mode performance," Opt. Lett. **30**(19), 2545–2547 (2005).
17. N. K. Fontaine, R. Ryf, S. G. Leon-Saval, and J. Bland-Hawthorn, "Evaluation of Photonic Lanterns for Lossless Mode-Multiplexing," in European Conference and Exhibition on Optical Communication, OSA Technical Digest (online) (Optical Society of America, 2012), paper Th.2.D.6.
18. N. K. Fontaine, R. Ryf, J. Bland-Hawthorn, and S. G. Leon-Saval, "Geometric requirements for photonic lanterns in space division multiplexing," Opt. Express **20**(24), 27123–27132 (2012).
19. A. M. Velazquez-Benitez, J. C. Alvarado, G. Lopez-Galmiche, J. E. Antonio-Lopez, J. Hernández-Cordero, J. Sanchez-Mondragon, P. Sillard, C. M. Okonkwo, and R. Amezcua-Correa, "Six mode selective fiber optic spatial multiplexer," Opt. Lett. **40**(8), 1663–1666 (2015).
20. B. Huang, N. K. Fontaine, R. Ryf, B. Guan, S. G. Leon-Saval, R. Shubochkin, Y. Sun, R. Lingle, Jr., and G. Li, "All-fiber mode-group-selective photonic lantern using graded-index multimode fibers," Opt. Express **23**(1), 224–234 (2015).
21. C. Okonkwo, R. van Uden, H. Chen, H. de Waardt, and T. Koonen, "Advanced coding techniques for few mode transmission systems," Opt. Express **23**(2), 1411–1420 (2015).
22. R. G. H. van Uden, C. M. Okonkwo, H. Chen, H. de Waardt, and A. M. J. Koonen, "Time domain multiplexed spatial division multiplexing receiver," Opt. Express **22**(10), 12668–12677 (2014).
23. N. Benvenuto and G. Cherubini, *Algorithms for Communications Systems and their Applications* (Wiley, 2002).
24. R. G. H. van Uden, C. M. Okonkwo, V. A. J. M. Sleiffer, H. de Waardt, and A. M. J. Koonen, "MIMO equalization with adaptive step size for few-mode fiber transmission systems," Opt. Express **22**(1), 119–126 (2014).
25. R. G. H. van Uden, C. M. Okonkwo, H. Chen, H. de Waardt, and A. M. J. Koonen, "28-GBd 32QAM FM transmission with low complexity phase estimators and single DPLL," IEEE Photonics Technol. Lett. **26**(8), 765–768 (2014).
26. R. G. H. van Uden, C. M. Okonkwo, V. A. J. M. Sleiffer, H. de Waardt, and A. M. J. Koonen, "Performance comparison of CSI estimation techniques for FMF transmission systems," in Photonics Society Summer Topical Meeting Series, Waikoloa, 2013.
27. B. Widrow and E. Walach, *Adaptive Inverse Control* (Wiley, 2008).

1. Introduction

Demand for more bandwidth continues at a phenomenal pace mainly attributed to emerging applications and services. In addition, the increased level of connectivity between devices is driving up bandwidth demand. A conservative range for the compounded annual growth rate

#240465 Received 11 May 2015; revised 31 Jul 2015; accepted 3 Aug 2015; published 11 Sep 2015

(CAGR) is expected to be between 20 and 40%. Even with a stabilizing CAGR, currently deployed single mode transmission systems are predicted to reach their capacity limits in the next decade [1]. Therefore, ongoing research in the field of space division multiplexing (SDM) is addressing the impending "capacity crunch" by exploring cost efficiently methods for extending the capacity of a single fiber with an additional multiplexing layer [2, 3]. More spatial channels can be created by adding single mode cores [4], increasing the number of guided modes [5] or a combination of both [6] within a single fiber. Here, we focus on a special type of multimode fiber, where a specific number of guided modes, limited by the fiber design can be addressed as individual channels. To date, impressive transmission results have been achieved by exploiting groups of linear polarized (LP) modes [7, 8]. However, further increasing the number of spatial mode channels has its challenges. As the number of guided mode groups is increased, a key challenge is managing the differential mode group delay, caused by the different propagation constant of the respective guided linear polarized modes. This can be ascertained from the impulse response associated with each mode. Hence, transmission over a high DMGD fiber requires larger processing effort in terms of the multiple input multiple output (MIMO) digital signal processing (DSP) required to unravel the mixed spatial channels, resulting in higher computational efforts and consequently, energy consumption at the receiver. Essential to keeping the computational complexity and energy consumption to a minimum are low DMGDs fibers [9]. In addition to DMGD, low mode dependent loss (MDL) is desired, as high MDL between spatial channels limits the theoretical throughput capacity of the system and increases the outage probability [9, 10]. Recently the transmission of 30 spatial channels over 23.8 km propagating the first 9 LP modes was reported [8]. However, high DMGD of 25 ns (~1 ns/km) and an MDL of 15-17 dB was reported. In this paper, we report a minimum DMGD of 0.2 ns (~0.05 ns/km) and maximum DMGD of 0.357 ns (~0.08 ns/km) after 4.45 km and MDL < 10 dB.

In this work, we address the novel key subsystems developed to demonstrate the first transmission of 20 spatial channels (2 polarizations per 10 spatial modes) over the 4.45 km of low DMGD 6-LP fiber. By transmitting 10 Gbaud QPSK per spatial channel a transmission rate of 400 Gbit/s per wavelength is realized. A gross system transmission rate of 2 Tbit/s is achieved by employing 5 wavelength channels. Accordingly, combined SDM and WDM transmission is presented. Furthermore, the overall system performance is optimized by a round-robin data encoder, which exploits the available spatial channels and allocates data across the channels in a round robin method. Accordingly, it minimizes the performance variance between all transmission channels.

Finally, by means of a ten-hour stability experiment, we demonstrate that the system bit error rate (BER) is below the 20% soft-decision forward error-coding (SD-FEC) limit of 2.4×10^{-2}, which is required for error free performance after error correction. During the experiment, the system MDL is measured to be around 8 dB with a maximum variation of 1.7 dB over 10 hours. This work demonstrates the potential of the 10 spatial mode fiber in offering higher density of spatial channels thereby increasing the capacity of a single fiber by a factor ten, with respect to conventional single mode fibers.

2. Low-DMGD 6-LP mode fiber

For the transmission of multiple modes, a desirable characteristic is low DMGD, as it limits the impulse response spread, which in turn limits the required memory in the receiver, and consequently reduces the DSP computational complexity at the receiver. Therefore, the employed fiber for this experiment is a 4.45 km 6-LP-mode fiber [11]. It is designed to guide the first 6 linearly polarized (LP) modes (10 spatial modes that can be divided into 4 mode groups, as illustrated in Fig. 1(a)), and to minimize the differential mode group delay and the bending losses. Note that an LP mode is a set of field modes with similar propagation constants. Accordingly, we depict the employed 6 LP modes, where their composition of true field modes, mode distribution and number of spatial and polarization channels are described

#240465 Received 11 May 2015; revised 31 Jul 2015; accepted 3 Aug 2015; published 11 Sep 2015

in Table 1. Since every field mode propagates in 2 polarizations, the aggregate number of available spatial and polarization channels in a 6-LP fiber is 20.

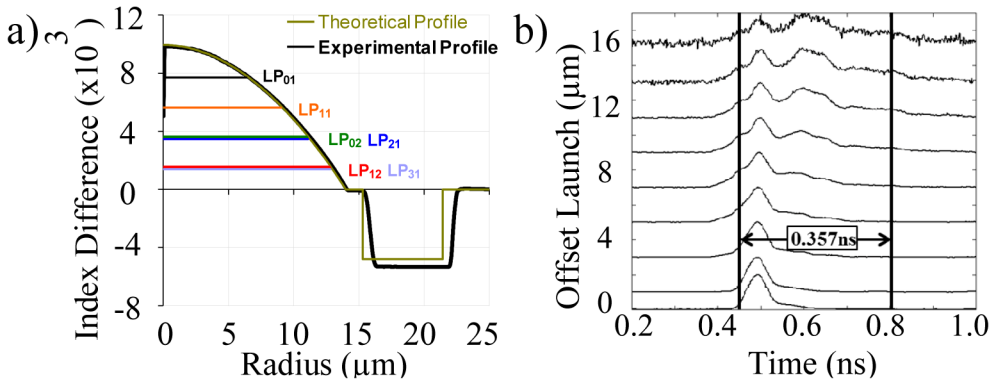

Fig. 1. a) Refractive index profile of the 6-LP mode fiber. b) DMGD plot of the 6-LP Mode fiber.

The higher order, undesired LP modes, are lossy due to the use of an optimized trench-assisted graded-index-core profile with the appropriate modal cut-off, which is depicted in Fig. 1(a). By first determining the core size, which directly relates to the normalized frequency V, this modal cut-off is optimized. To guide up to 6-LP modes, V is 9.65. The corresponding core radius is 15 μm. Next the trench volume (integral of the trench index relative to the cladding over its cross-section) can be chosen such that it minimizes the bend losses. The higher order modes are generally more sensitive to bending losses. Finally the alpha parameter, relating to the shape of the refractive index arc of the graded-index core is adjusted to minimize the DMGD between any 2 LP modes.

Table 1. The 6LP modes formed by field modes, where red and blue correspond to the positive and negative phase, respectively. The number of spatial channels includes linear polarizations of the spatial LP modes.

Mode group	Mode distribution	Field Modes	Number of spatial channels (aggregate)
LP01		HE11	2
LP11		HE21, TE01, TM01	4 (6)
LP21		EH11, HE31	4 (10)
LP02		HE12	2 (12)
LP31		EH21, HE41	4 (16)
LP12		HE22, TE02 TM02	4 (20)

<graphic> </graphic>

Key to the design of low DMGD fibers is the sensitivity to small refractive index variations, and changes in the alpha parameter in particular. Note that a variation of 1% in alpha, which is in line with conventional manufacturing tolerance, increases the minimum theoretical DMGD value by a factor of 11.5, from 8.6ps/km to 98.5ps/km [11]. To match the designed index profile closely, the fiber is fabricated using high accuracy plasma chemical vapor deposition (PCVD). It has standard glass (125 μm) and coating (245 μm) dimensions. The DMGDs between the 6 guided LP modes were measured by offset launching to be ≤ 80

#240465 Received 11 May 2015; revised 31 Jul 2015; accepted 3 Aug 2015; published 11 Sep 2015

ps/km at 1550 nm, yielding a delay spread ≤ 0.357 ns over 4.45 km (Fig. 1b). The chromatic dispersion is between 19 and 21 ps/nm/km, and the effective areas were above 115 μm^2 (from ~117 and ~270 μm^2), which ensures low intra-mode nonlinearity. Finally, the attenuation of the fundamental LP_{01} mode was measured at 0.207 dB/km at 1550 nm, and the difference in the attenuation between the modes was estimated to be < 0.01 dB/km, which limits MDL. Note that a 9-LP-mode fiber made with PCVD and with DMGDs <155ps/km has recently been reported [12], demonstrating the ability of this profile and process to increase the number of modes that can be supported by a few-mode fiber.

3. Low loss all fiber photonic lanterns

To address the spatial mode channels, a mode multiplexer (MMUX) is required. To date, various techniques such as phase plates [5], 3-dimensional waveguides [6, 13, 14] and all-fiber photonic lanterns (PL) have been demonstrated [15–20]. Advantages of the latter are low loss, low MDL and high temporal stability. For these reasons all-fiber photonic lantern are investigated for this system.

The employed PL is fabricated using 10 single mode fibers with a core diameter of 13 µm, and are placed inside a low refractive index glass capillary. The fibers are accurately positioned to match the modal symmetry and prevent high losses [18]. To achieve the geometry required to launch the 10 modes, the 3 inner SMFs (86 µm cladding diameter) are surrounded by 7 larger SMFs (125 µm cladding diameter), as illustrated on the left hand side of Fig. 2 [18]. The flourine-doped silica capillary is then adiabatically tapered down from 900 µm to 57 µm within a transition length of 5.75 cm. The tapered facet of the PL is shown in Fig. 2 on the right inset image, and has an inner diameter of 28 µm, which matches to the 6-LP fiber dimensions and mode-fields as described in section 2.

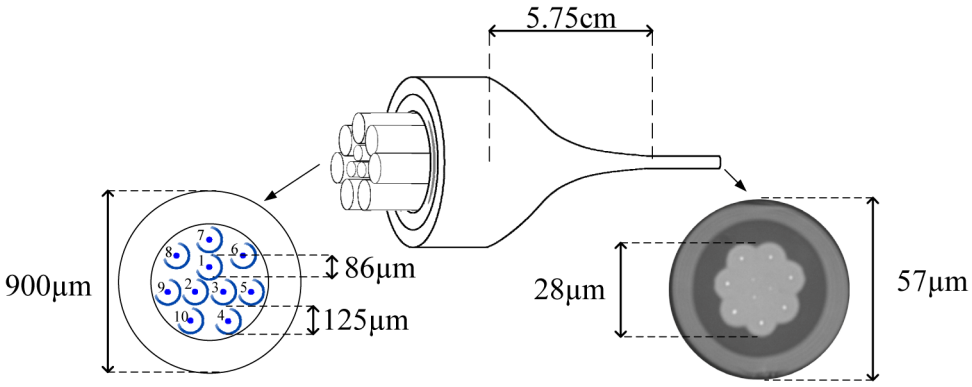

Fig. 2. Photonic lantern: Schematic of the fiber geometric arrangement to achieve the adiabatically tapered coupler and the resulting end facet of the 10 mode photonic lantern. Depicting the SMF core (86 and 125 µm), outer diameter of the front facet (900 µm), inner (28 µm) and outer (57 µm) diameter of the end facet, and the tapering length (5.75 cm).

By consecutively addressing the individual ports and observing the PL output with an infrared camera (Xenics, XEVA-1.7-320), characterization of the near field intensity profiles is performed. As shown in Fig. 3, notice that due to the non mode selectivity of the PLs, no discernable mode fields are visible for the near field mode profiles taken at 1550 nm, using a 50 nm bandwidth light source. With a DFB laser at 1540 nm and an integrating sphere detector, the excess losses of the ports have been measured. In addition, to fully capture the power of all modes and test port-by-port coupling losses, a graded index multimode fiber with core diameter 50 µm was butt-coupled to the PL for measurement.

#240465 Received 11 May 2015; revised 31 Jul 2015; accepted 3 Aug 2015; published 11 Sep 2015

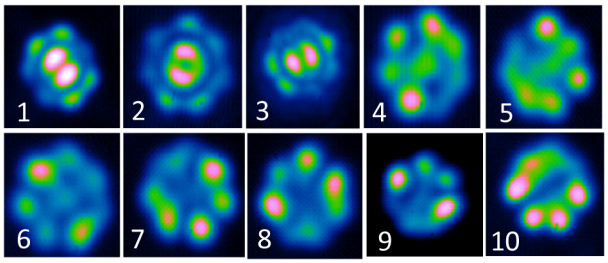

Fig. 3. Near field mode profiles measured at the output facet for each port of the non mode-selective photonic lantern.

In both measurements, the power launched into the lantern is 0 dBm. The loss measurement results are depicted in Fig. 4. From the excess losses, the MDL of the photonic lantern is estimated to be approximately 2 dB. The loss difference between the ports is partially attributed to alignment and connector losses.

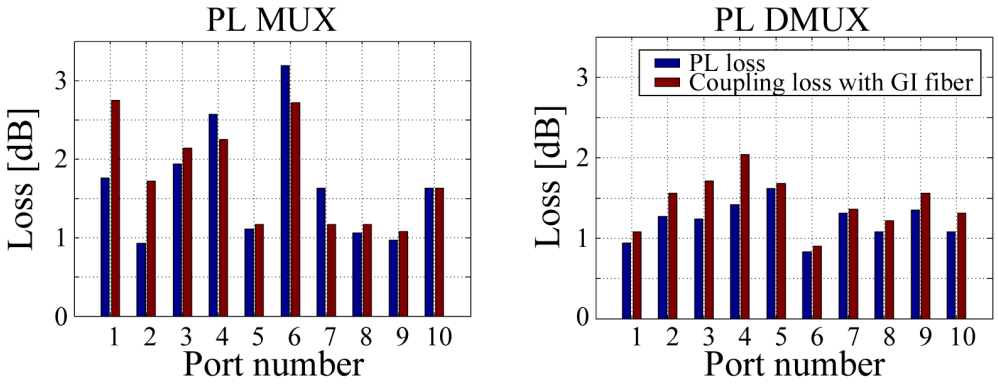

Fig. 4. Loss of the PL and coupling losses into 50µm GI fiber for MUX and DMUX PL.

4. Experimental setup

4.1 Transmitter side

The experimental setup is depicted in Fig. 5a. At the transmitter, external cavity lasers (ECL) are used to generate 50GHz spaced wavelength channels centered on 1547.72 nm. The channels are modulated with a 10 GBaud QPSK pseudo random bit sequence (PRBS) of length 2^{15} using an IQ modulator driven by two synchronized digital analog converters (DACs). This sequence is generated using a novel round-robin (RR) encoder which is based on a space-time code [21]. The round-robin coding averages the overall system performance by allocating time slots of data channels over all the transmitted spatial channels. In this setup data channel $0 \le m \le 19$ is allocated to transmission channel $0 \le n \le 19$ at time slot $0 \le k \le \infty$ as $n = \mathrm{mod}_{20}(m + k)$, where mod_{20} is the modulus after division by 20 function. Figure 5b provides a graphical representation of the round robin coding scheme. It is important to note that the theoretical implication is small, however the hardware considerations for potential implementation are challenging due to timing implications. Critical timing alignment is required at the transmitter and receiver side for decoding the channels in DSP.

The output of the modulator is connected to a polarization multiplexing stage, where the polarizations are split and one arm is delayed by 485 ns before being recombined for transmission. The same principle is applied to decorrelate the wavelength channels. A wavelength selective switch (WSS) separates the odd and the even wavelength channels. The odd channels are delayed by 985 ns before both are recombined. This output is then split into 10 dual polarization (DP) signals, and each is further delayed to create the required 10 fully

#240465 Received 11 May 2015; revised 31 Jul 2015; accepted 3 Aug 2015; published 11 Sep 2015

decorrelated signal copies to address all spatial mode channels. The corresponding delays are given in Fig. 5a. Note that erbium doped fiber amplifiers (EDFAs) are used to compensate for the splitting losses and to manage and optimize the launch powers for the mode channels. An ideal setup would have 10 independent amplifiers to minimize the differential losses between launch ports. However, to limit the number of amplifiers employed in the experiment, one EDFA is used to amplify 2 mode signals (Fig. 5a.). All signals are coupled in to the 6-LP mode fiber described in section 2 using the lantern from section 3.

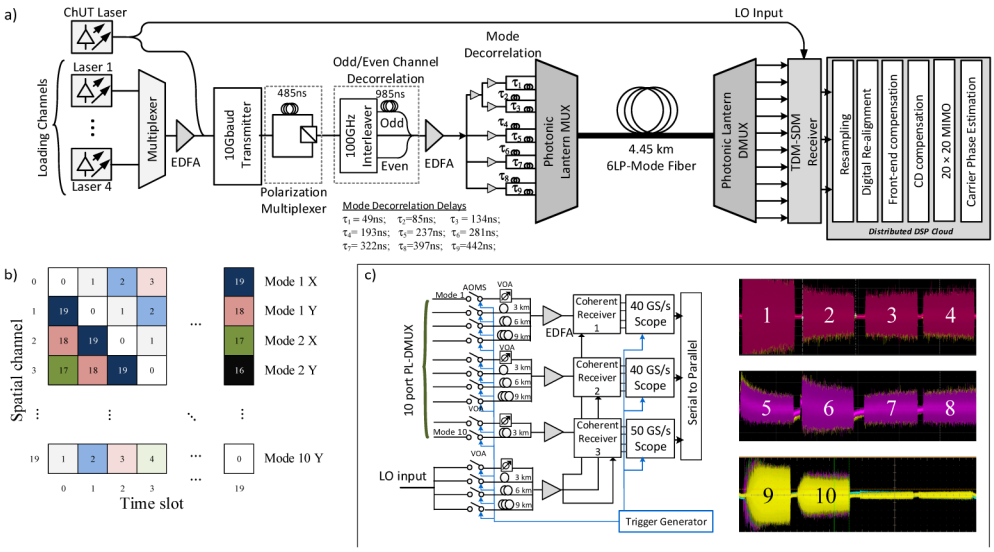

Fig. 5. a) Experimental transmission setup. b) Graphical representation of the round-robin coding scheme. c) TDM-SDM receiver and corresponding oscilloscope displays depicting 10 modes.

4.2 Receiver side

At the receiver side, a reciprocal setup as the transmitter side is used to demultiplex the mixed 10 mode DP signal. The PL outputs are connected to a TDM-SDM receiver (Fig. 5c) [22]. In this setup outputs corresponding to spatial channels 2, 3 and 4 are temporally separated using a fiber of 3, 6, and 9 km respectively, before being combined to a single output and thus allocating the 4 spatial channels into 4 different time slots. The time-multiplexed signals are amplified to compensate the losses in the TDM-SDM, before being captured by a coherent receiver and a real time oscilloscope. Similarly, by employing a TDM-SDM block for spatial channels 5, 6, 7 and 8 and another block for 9 and 10, only 3 coherent receivers and corresponding real time oscilloscopes are required to receive 10 modes. The three scopes are synchronized by a trigger and have a sample rate of 40 GS/s or 50 GS/s. A screen capture of the oscilloscopes during a 10 mode measurement is depicted in Fig. 5c. Blocks 5 to 10 show switching transients of the trans-impedance amplifier (TIA) of the coherent receivers. As every block has a length of 12.5 µs (500k samples at 40 GS/s) and the transmitted sequence is repeated every 3.3 µs (2^{15} symbols at 10 GBaud), the first samples influenced by this unwanted transient can be discarded while enabling accurate BER estimations. To keep the local oscillator (LO) within coherence and thus minimize experimental complexity, the LO path is matched to the signal delays.

Before any signal processing can be performed, the captured blocks must be re-aligned in the digital domain. The data is then parallel processed offline in a distributed DSP cloud, where it is down sampled to 20 GS/s and optical front-end impairments are compensated. Unraveling the 20 data channels is achieved using a 20x20 minimum mean squared error

#240465 Received 11 May 2015; revised 31 Jul 2015; accepted 3 Aug 2015; published 11 Sep 2015

(MMSE) time domain equalizer (TDE). With respect to TDE, a frequency domain equalizer (FDE) can reduce the computational complexity [23]. However, TDE is employed in this work due to the available capture window (which is intrinsically limited by the fiber lengths employed for the 10 spatial mode TDM-SDM receiver). Due to the lower adaptation gain FDE is too slow for stabile convergence while still maintaining enough symbols for accurate BER analysis. The weight matrix uses the least means squares (LMS) update algorithm for convergence, and switches after 40k symbols to decision directed least means squares (DD-LMS). Both algorithms have variable step-sizes [24]. In order to corroborate the impact of impulse response changes during the change from data-aided to decision-directed mode, we reprocessed a capture without any updates to the weight matrix after 40k symbols. Our results from this test, showed that after initial convergence, the BER values remains the same. Furthermore, we observed stable BER for multiple captures. From this we can conclude that the impulse response is stable for the used capture length.

Subsequently, the small frequency offset between transmitter and LO is removed by applying carrier phase estimation based on digital phase locked loops [25]. Next, the symbols are demapped. Note that symbols used for convergence are removed before the bit error rate (BER) is calculated over the remaining 100k symbols per channel. The system BER is the average of all channels and thus averaged over 4million bits. Finally, the maximum mode dependent loss between any 2 modes is calculated by taking the ratio between the highest and lowest eigenvalue of the TDE weight matrix [26]. The calculated MDL is an estimation for the full system. Except for the MDL estimations from the loss measurement for the lanterns, the MDL for individual components could not be measured.

5. Results

First, the system is operated back-to-back to determine the optimal signal and oscillator power for the receivers. Next, the photonic lanterns and FMF are placed in the setup for the 10-mode measurement.

The low DMGD of the fiber is best visualized by the impulse response of the system. For clarity, it is not possible to display all 400 weight elements, therefore the average of all elements is calculated and shown in Fig. 6. This graph indicates a minimum delay spread of < 0.2 ns after 4.45 km transmission. The delay spread is in agreement with the low DMGD values measured by offset launching at fiber manufacture shown in Section 2 (Fig. 1b). Observe that the average impulse response can be improved when the number of samples captured is increased. Due to small mismatch in the timing re-alignment of the TDM-SDM receiver setup, the impulse response peak deviates by at most 50 ps. However, we highlight that this has negligible influence on the performance of the system.

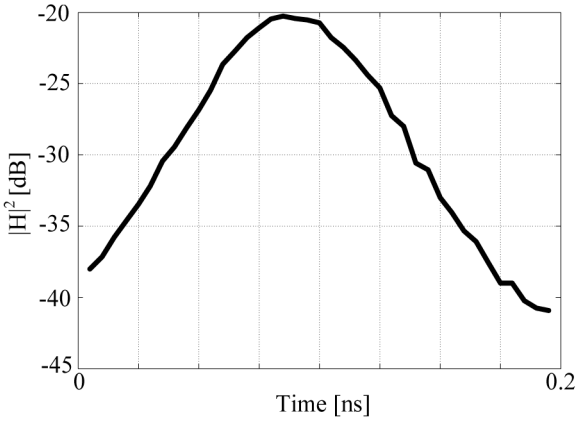

Fig. 6. Average time domain equalizer weight response of the 20 x 20 MIMO elements.

#240465 Received 11 May 2015; revised 31 Jul 2015; accepted 3 Aug 2015; published 11 Sep 2015

Furthermore the convergence of the 10-mode measurement is compared with a back-to-back single mode convergence in Fig. 7. Both cases uses 39 double symbol rate taps and an adaptation gain $\mu = 10^{-4}$. For the sake of comparison, the error is normalized such that the initial error is 1 and the final value is 0, and system convergence is considered when the error is within 5% of the final value. The graph indicates that all the spatial channels converge at the same rate and reaches the convergence threshold after 0.58 μs. This is approximately a factor 11 slower compared to the SMF transmission, which takes only 0.05 μs to converge. This is as expected from theory, as the convergence time scales linearly according to the number of mixed transmission channels [27]. The small discrepancy is attributed to the eigenvalue spread of the transmission system.

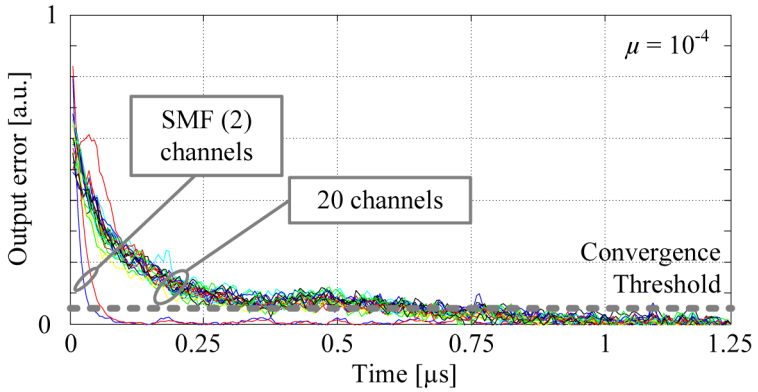

Fig. 7. TDE error convergence over time for the 6-LP Mode fiber and B2B SMF.

Figure 8 shows the bit error rates of all the channels as well as the error rate after applying the round robin coding scheme. To emphasize the difference in performance of all spatial channels, the constellations of the worst and best performing channels are depicted (inset of Fig. 8). This difference in channel performance is correlated with the coupling between the photonic lanterns and fiber. Due to the coupling efficiency, the diversity of the receiver is not fully exploited, resulting in higher bit error rates in some of the spatial channels. Observe the difference in the performance of each polarization in Fig. 8. We attribute this to the polarization dependent loss in the system, mainly introduced from the polarization multiplexing stage (where a non-polarization maintaining fiber is employed for the decorrelation delay between the two polarization arms) and the launching conditions.

Without round-robin coding, the system performance is limited to the worst performing channel (Fig. 8). In this case, transmission performance is poor, as the BER of that channel is above the FEC limit. By introducing the RR coding scheme, the system BER averages over all channels, reducing the system BER from 5.2×10^{-2} to 1.4×10^{-2}, and so enabling transmission in this experiment below the 20% SD-FEC limit.

#240465 Received 11 May 2015; revised 31 Jul 2015; accepted 3 Aug 2015; published 11 Sep 2015

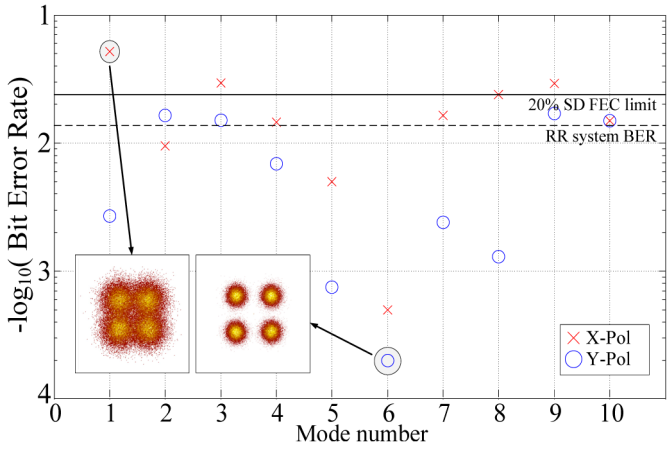

Fig. 8. Round-robin coding system BER, individual channel BER and constellations of the best and worst performing channels.

Finally, we perform a WDM experiment to achieve the gross transmission rate of 2 Tbit/s by combining WDM and SDM. The 5 wavelengths are centered on 1547.72 nm and spaced at 100 GHz. Figure 9 indicates successful transmission as all transmitted channels perform below the 20% SD-FEC limit. The measured MDL values for the channels (ordered short to longer wavelength) are 8.7, 9.3, 9.0, 9.4, and 9.5 dB, and follows the same trend as the bit error rate.

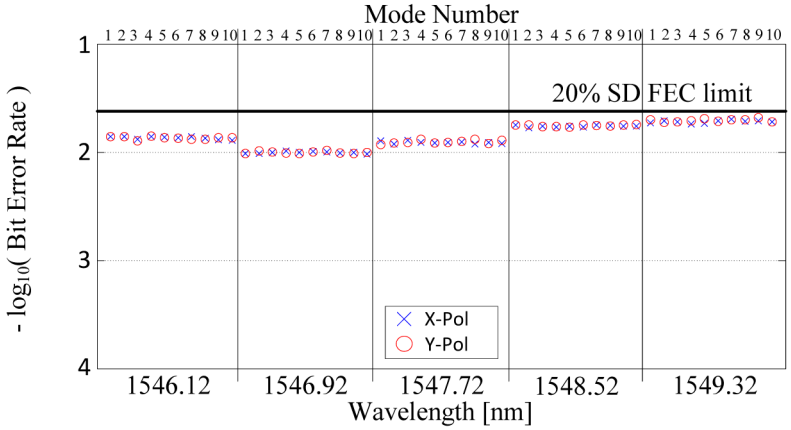

Fig. 9. BER for 5 wavelength channels ranging from 1546.12 nm to 1549.32 nm.

Furthermore, a key validation of transmission systems is long-term reliability, which was verified by performing a long term measurement over 10 hours with all 5 wavelengths enabled. Figure 10 shows the BER performance over 10 hours (10 minute intervals) of the center channel (1547.72 nm), and from the figure a minimal variation of 1.1 × 10-2 in the BER can be observe, demonstrating the stability of the transmission system. The MDL is also shown to be stable and is measured to be around 8.5 dB with a maximum variation of 1.7 dB.

#240465 Received 11 May 2015; revised 31 Jul 2015; accepted 3 Aug 2015; published 11 Sep 2015

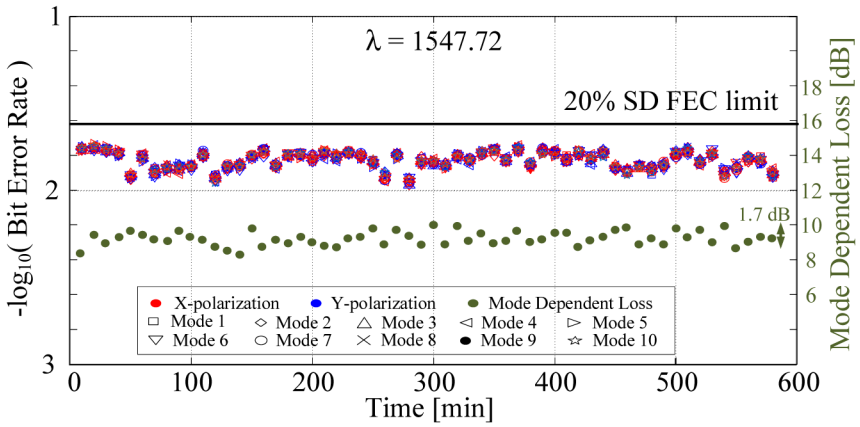

Fig. 10. Long term 20 spatial channel BER and MDL measurement over 10 hours.

6. Conclusion

By employing low-loss, all fiber photonic lanterns to launch into a 4.45km low DMGD 6-LP fiber, we demonstrate the first 10 mode transmission system. In addition the record minimum DMGD of 0.2 ns (max. 0.357 ns) after 4.45 km has been measured. The low DMGD offers the potential for scaling to longer transmission distances without adding to the impulse response length. Finally, long-term stability of multi wavelength, multi-mode transmission system has been verified, using the suggested round-robin coding to increase system performance by equalizing spatial inter-channel performance. This work demonstrates a high density single core spatial division multiplexed transmission offering a 10-fold increase in single core fiber capacity. Therefore, we envisage that the continual growth in service driven demands for more capacity can be delivered.

Acknowledgment

We gratefully acknowledge partial funding from EU FP7-ICT MODE-GAP project (grant agreement 258033), and ARO grant W911NF-13-1-0283. Micram Instruments and Tektronix are gratefully acknowledged for help with digital-to-analog converters and real-time scopes respectively.

#240465 Received 11 May 2015; revised 31 Jul 2015; accepted 3 Aug 2015; published 11 Sep 2015